

# **Hypoxia drives breast tumor malignancy through a TET -TNF $\alpha$ -p38-MAPK signaling axis**

Min-Zu Wu<sup>1</sup>, Su-Feng Chen<sup>2,3</sup>, Shin Nieh<sup>3</sup>, Christopher Benner<sup>4</sup>, Luo-Ping Ger<sup>5,6</sup>,  
Chia-Ing Jan<sup>7</sup>, Li Ma<sup>1</sup>, Chien-Hung Chen<sup>1</sup>, Tomoaki Hishida<sup>1</sup>, Hong-Tai Chang<sup>8</sup>,  
Yaoh-Shiang Lin<sup>9,10</sup>, Nuria Montserrat<sup>11</sup>, Pedro Gascon<sup>11</sup>, Ignacio Sancho-Martinez<sup>1</sup>,  
and Juan Carlos Izpisua Belmonte<sup>1,\*</sup>

<sup>1</sup>Gene Expression Laboratory, Salk Institute for Biological Studies, La Jolla,  
California, USA

<sup>2</sup>Department of Dental Hygiene, China Medical University, Taichung, Taiwan

<sup>3</sup>Department of Pathology, National Defense Medical Centre and Tri-Service General  
Hospital, Taipei, Taiwan

<sup>4</sup>Integrative Genomics and Bioinformatics Core, Salk Institute for Biological Studies,  
La Jolla, California, USA

<sup>5</sup>Institute of Biomedical Sciences, National Sun Yat-Sen University, Kaohsiung,  
Taiwan

<sup>6</sup>Department of Medical Education and Research, Kaohsiung Veterans General  
Hospital, Kaohsiung, Taiwan

<sup>7</sup>Department of Pathology, China Medical University and Hospital, Taichung, Taiwan

<sup>8</sup>Department of Surgery, Kaohsiung Veterans General Hospital, Kaohsiung, Taiwan

<sup>9</sup>Department of Otolaryngology–Head and Neck Surgery, National Defence Medical  
Centre and Tri-Service General Hospital, Taipei, Taiwan

<sup>10</sup>Department of Otolaryngology–Head and Neck Surgery, Kaohsiung Veterans  
General Hospital, Kaohsiung, Taiwan

<sup>11</sup>Department of Medical Oncology, Hospital Clinic Barcelona, Barcelona University,  
Barcelona, Spain

M.-Z. Wu and S.-F. Chen contributed equally to this article.

*Running title:* Hypoxia drives breast tumor malignancy

*Keywords:* breast tumor initiating cells; hypoxia; TNF $\alpha$ -p38-MAPK; DNA  
hydroxymethylation; TET

## **Disclosure of Potential Conflicts of Interest**

No potential conflicts of interest were disclosed.

## **Precis**

Results shed new mechanistic light on how the hypoxic tumor microenvironment  
affects the epigenetic programs in cancer cells to drive stem-like character and

metastatic development, suggesting new ways to eradicate cancer stem-like cells that are nurtured by such microenvironments.

## **Abstract**

Hypoxia is a hallmark of solid tumors that drives malignant progression by altering epigenetic controls. In breast tumors, aberrant DNA methylation is a prevalent epigenetic feature associated with increased risk of metastasis and poor prognosis. However, the mechanism by which hypoxia alters DNA methylation or other epigenetic controls that promote breast malignancy remains poorly understood. We discovered that hypoxia deregulates TET1 and TET3, the enzymes that catalyze conversion of 5-methylcytosine (5mC) to 5-hydroxymethylcytosine (5hmC), thereby leading to breast tumor initiating cell (BTIC) properties. TET1/3 and 5hmC levels were closely associated with tumor hypoxia, tumor malignancy and poor prognosis in breast cancer patients. Mechanistic investigations showed that hypoxia leads to genome-wide changes in DNA hydroxymethylation associated with upregulation of TNF $\alpha$  expression and activation of its downstream p38-MAPK effector pathway. Coordinate functions of TET1 and TET3 were also required to activate TNF $\alpha$ -p38-MAPK signaling as a response to hypoxia. Our results reveal how signal transduction through the TET-TNF $\alpha$ -p38-MAPK signaling axis is required for the acquisition of BTIC

characteristics and tumorigenicity in vitro and in vivo, with potential implications for how to eradicate BTIC as a therapeutic strategy.

## **Introduction**

Breast cancer is the most common malignancy among women and exhibits a high rate of heterogeneity (1). Although mortality of patients with breast cancer in recent years has significantly decreased, tumor malignancy of breast cancer still leads to a poor prognosis and limits therapeutic options. It was proposed that tumor initiating cells (TICs), defined by their abilities for tumor-forming and self-renewing, account for tumor malignancy (2). Recently, the population of TICs has been identified in numerous tumors including those of brain, head and neck, and lung cancer through various molecular markers, side population and enzyme activity (3-5). Likewise, breast tumor initiating cells (BTICs) have been isolated by sorting for CD44<sup>High</sup>/CD24<sup>Low</sup> cells, high aldehyde dehydrogenase1 (ALDH1) activity or enriched in anchorage-independent conditions (6-8). They were found to share a high degree of similarity of characteristics with stem cells as well as tumorigenic capacity (9). High content of BTICs are enriched with high grade of breast tumor and associated with enhanced invasiveness, chemoresistance, and metastasis (10), supporting the concept that BTICs account for tumor malignancy of breast cancer (11).

Hypoxia, a microenvironment stress existing in various solid tumors, has been recognized as an important factor promoting tumor malignancy (12). Recent reports demonstrating the association of hypoxia with high-grade breast tumor and poor prognosis of patients with breast cancer have suggested an important role for hypoxia in breast cancer (13). Noticeably, hypoxia has been demonstrated to be associated with a stem-like phenotype in breast cancer and provides a breeding ground for BTICs (14). This is consistent with the fact that TICs are supported by their niche where they are regulated by complex interactions with multiple factors derived from the tumor microenvironment (15).

One key mechanism by which hypoxia regulates tumor malignancy is alteration of the cancer epigenome, which provides selective advantages for cancer cells during tumorigenesis (16-17). Aberrations in DNA methylation and proteins involved in controlling DNA methylation are associated with tumor malignancy and prognosis of patients (18). However, the mechanism by which hypoxia regulates DNA methylation and key enzymes in regulating tumor malignancy remains largely unknown. The Ten-Eleven Translocation (TET) family of enzymes convert 5-methylcytosine (5mC) to 5-hydroxymethylcytosine (5hmC) for the demethylation of mammalian DNA (19).

The TET family comprises three members: TET1, TET2 and TET3. The *TET1* gene was firstly identified as a fusion partner of MLL in acute myeloid leukemia associated with a chromosome translocation. The expression of TET1 is required for ESC pluripotency and normal differentiation during ESC lineage specification (20). TET2 plays an important role in hematopoiesis. Loss of function of TET2 has been reported as one of the most frequent genetic defects in myeloid malignancies (21). In addition, TET3, but not TET1 or TET2, highly expressed in oocytes and zygotes, is essential for epigenetic reprogramming of the zygotic paternal DNA (22). Despite these findings suggest critical roles that TET family proteins play during biological processes, it is unclear whether TET proteins act as key factors in regulating hypoxia enhanced tumor malignancy as well as tumor initiating capabilities.

In this study, we reveal an epigenetic mechanism centered on hypoxia induced activation of the TNF $\alpha$ -p38-MAPK signaling axis leading to breast tumor malignancy, and highlight that TET1/3 and 5hmC might serve as prognostic biomarkers for breast cancer. The inhibitory effect of blocking the TET-TNF $\alpha$ -p38-MAPK signaling pathway on BTIC characteristics and tumorigenicity indicates a potential strategy to improve targeted therapy in breast cancer.

## **Materials and Methods**

### ***Cells, plasmids, stable transfection and oxygen deprivation***

Primary breast cancer cells were obtained from surgical specimens of patients with breast cancer. This study was approved by the Institutional Review Board of the Tri-Service General Hospital, Taipei, Taiwan. The primary cells were maintained in Dulbecco's Modified Eagle's Medium (DMEM) supplemented with 10% FBS and 1% penicillin/streptomycin. MCF7 and MDA-MB-231 cell lines were cultured in the DMEM medium supplemented with 10% FBS at 37°C in the presence of 5% CO<sub>2</sub>. A pBabe-HIF-1α P402A/P564A (addgene) plasmid was used in generating HIF-1α overexpression clones. The plasmids for gene knockdown experiments were generated by construction of an oligonucleotide targeting a specific gene sequence into pSUPER vector (oligoengine), which were subjected to establish stable transfectants. The target sequences in the experiments are listed in Supplementary Table S2. Oxygen deprivation was conducted in the hypoxic incubator with 1% O<sub>2</sub>, 5% CO<sub>2</sub> and 94% N<sub>2</sub> for 24 h.

### ***Patient selection***

This research followed the tenets of the Declaration of Helsinki and was approved by the Cardinal Tien Hospital institutional review board. All samples were obtained from patients after informed consent. Tissue specimens from 183 patients were obtained from radical surgical resections with human breast carcinoma. A retrospective study of patients selected from a clinical database from the archives of the Department of Pathology, Cardinal Tien Hospital between 1998 and 2005. Eighteen patients either without follow-up or insufficient clinicopathological data for analysis were excluded. Therefore, only 165 cases of human breast carcinoma were included in this study.

### ***Immunohistochemistry (IHC)***

IHC was performed on 165 archived, formalin-fixed, paraffin-embedded (FFPE) blocks of breast IDCs. Tissue sections were de-waxed in xylene and rehydrated in alcohol, followed by incubation in 0.01 M citrate buffer pH 6.0 at 95°C for 40 min in a water bath. They were then treated with 0.3% H<sub>2</sub>O<sub>2</sub> for 30 min to block endogenous peroxidase; and incubated with block non-specific antibody reactions. All the slides were counterstained with haematoxylin (Merck, Darmstadt, Germany). Antibodies used in the experiments are listed in Supplementary Table S3.

### ***Immunohistochemical staining evaluation***

The histopathological slides of all the specimens were reviewed concurrently and independently by two expert pathologists using the same type of microscope without prior knowledge of each patient's clinical details. To evaluate precisely and objectively the intensity of 5hmC, TET-1, TET-3 and HIF-1  $\alpha$  staining, we used a Zeiss AxioImager-Z1 microscope to capture images of all sections, and measured the intensity of staining for the four markers using Program Metamorph software. Intensity was classified into four categories: no staining scored 0, fewer staining scored 1, less than average intensity (low intensity) scored 2, and higher than average (high intensity) scored 3. The mean immunoreactivity score of each marker was selected as the cut-off point to separate tumors showing negative ( $\leq$ mean) and positive ( $>$ mean) expression. The correlation between expression levels of specific factor and tumor grade was calculated as described previously (23).

### ***Western blot analysis, RNA extraction, quantitative real-time PCR***

Western blot was performed following a standard protocol as described previously (16). Briefly, cells were harvested and lysed by RIPA buffer (50mM Tris, 150mM NaCl, 0.1% SDS, 0.5% Deoxycholate, 1% NP-40). Protein extracts were subjected to

SDS-PAGE analysis. The membranes were blocked with 5% nonfat milk followed by antibody hybridization and the signals were visualized on X-ray film. For RNA extraction, total RNAs from cultured cells were extracted using the Trizol reagent (Invitrogen Life Technologies), and 1  $\mu$ g of RNA was used for cDNA synthesis. Quantitative real-time PCR was carried out to quantify gene expression level by using the CFX384 Touch Real-Time PCR Detection System (BIO-RAD Laboratories, Inc.). The primers and antibodies used in the experiments are listed in Supplementary Tables S2 and S3, respectively.

#### ***Luciferase reporter assays***

Cells were seeded onto 6-well plates and transfected with the following: reporter plasmid containing TET1 or TET3 gene promoter with wild type or mutated hypoxia response element, internal control plasmid encoding  $\beta$ -gal, and expression vector encoding wild type HIF-1 $\alpha$ . Transfected cells were exposed to 20% or 1% O<sub>2</sub> for 24 h. Firefly luciferase activities in cell lysates were measured using Luciferase Assay System (Promega) and  $\beta$ -gal activities were used as an internal control for data normalization.

#### ***ELISA assay***

Cells were seeded on 6 well plates at an equal density and incubated for 24 hr. Then, cells were further incubated for 24 hr with serum-free DMEM medium in normoxia or hypoxia. The collected supernatants were subjected to ELISA assay following the standard protocol as described in the instruction of the ELISA Kit (eBioscience). ELISA assays were performed in duplicate three separate times, and the data are expressed as mean  $\pm$  SD.

#### ***qPCR-ChIP, hMe-DIP and hMe-DIP-seq***

qPCR-ChIP assay was performed following a standard protocol as described previously (16). Briefly, crosslinked cell lysate was sonicated and subjected to immunoprecipitation reaction. The immunoprecipitated DNA was purified through a phenol-chloroform DNA extraction protocol and then subjected to qPCR analysis. The hMe-DIP assay was performed as described previously. Briefly, genomic DNA was prepared with genomic DNA extraction kit (Promega) and sonicated into fragments ranging ~500bp. The fragmented DNA was denatured for 10 min at 95°C and immunoprecipitated overnight at 4°C with anti-5hmC antibody (Active Motif) in 500  $\mu$ l IP buffer (10 mM sodium phosphate, 140 mM NaCl, 0.05% Triton X-100). DNA was eluted from the beads followed by purification with chromatin IP DNA purification kit (Active Motif). For hMe-DIP-seq, genomic DNA was purified and

sonicated. Illumina barcode adapters were ligated before hMeDIP. Adaptor-ligated DNA was denatured, followed by incubation with 5-hmC antibody (Active Motif). The immunoprecipitated DNA was purified and sequenced followed by standard Illumina protocols. hMeDIP reads were mapped to the human genome (hg19, GRCh37) using bowtie2 (24). Only reads that map uniquely to the genome were used for downstream analysis (MAPQ > 10). HOMER was used to generate normalized bedGraphs for the UCSC Genome Browser (25). Both hMeDIP-seq and TSS-Seq read depths at promoter regions were calculated using HOMER, and significant differentially regulated promoters were determined using EdgeR (26). Hi-C analysis and calculation of PC1 values were carried out by HOMER as previously described (27). Gene ontology term analysis was performed by database for annotation, visualization, and integrated discovery (DAVID) programs.

### ***Orthotopic transplantation assays***

Animal studies were approved by the Institutional Review Board of the Salk Institute for Biological Studies, La Jolla, U.S.A. Cells were trypsinized and resuspended in PBS/Matrigel (1:1; BD Biosciences). Suspended cells were then transplanted into the mammary fat pad of a young (3-4 weeks) nude female mouse. Before injection of suspended cells, the abdominal skin of mice was opened by a

Y-shaped incision. The incision was made around the fourth nipple. After incision, the skin was folded back to expose the mammary fat pad where suspended cells were injected. Tumor incidence was monitored by using an *in vivo* imaging system. After 10 weeks, all of the tumors were collected and animals were sacrificed.

### ***Statistical analysis***

$\chi^2$  tests (with Fisher's exact test when expected value <5 in >20% table cells) were used to measure the significance between nominalized 5hMC, TET-1, TET-3 and HIF-1 $\alpha$  intensity of immunoreactivity and distribution percentages as well as clinicopathological characteristics. The associations between 5hMC, TET-1, TET-3 and HIF-1 $\alpha$  scores and clinicopathological multivariables were calculated by the Kruskal–Wallis *H*-test with Bonferroni multiple comparison procedure. The Kaplan–Meier method was used to obtain survival curves. SPSS software v.15.0 (SPSS UK Ltd, Woking, UK) was used for the analysis. All data were reported as mean  $\pm$  SD. Statistical analysis was performed by using Student's *t* test and  $p < 0.05$  was considered significant.

### ***Accession number***

Sequencing data have been deposited to the Gene Expression Omnibus (GEO)

under accession number GSE60434

## Results

### Hypoxia induces tumor initiating characteristics in breast cancer cells

Recent findings suggest that hypoxia results in the acquisition of stem cell-like tumor initiating phenotypes, which are associated with tumor malignancy (14,28). Thus, we first investigated whether similar phenotypes could be recapitulated by hypoxia in breast cancer. We found that hypoxia resulted in the acquisition of putative breast tumor initiating cell (BTIC) phenotypes reported previously (7-8,29), including the appearance of a CD44<sup>+</sup>/CD24<sup>-</sup> population, an increased ALDEFLUOR-positive (ALDH<sup>+</sup>) population and the upregulation of genes related to stemness in primary cultures from patients with breast cancer as well as breast cancer cell lines, MCF7 and MDA-MB-231 cells (Fig. 1A-F). Likewise, increased mammosphere forming capacity, a phenotypic characterization of BTICs, was observed in hypoxic primary cells and breast cancer cell lines (Fig. 1G). As expected, stable overexpression of a constitutively active form of HIF-1 $\alpha$  consistently recapitulated these phenotypes in breast cancer cell lines (Supplementary Fig. S1). As putative BTICs have been found to reside within a CD44<sup>High</sup>/CD24<sup>Low</sup> population (7), thus we sorted CD44<sup>+</sup>/CD24<sup>-</sup>

subpopulations from cells in which HIF-1 $\alpha$  was stably overexpressed (Supplementary Fig. S2A). Upon characterization of the sorted cells (hereafter referred to as isolated BTICs) we found that these cells expressed canonical BTIC phenotypes (Fig. S2B-D and Fig. S1D, see also in Fig. 4H). Next, we examined whether these isolated BTICs undergo the Epithelial-Mesenchymal Transition (EMT) process, given that it has been identified as a feature of BTICs (30). Western blot analysis demonstrated that the EMT process was induced in isolated BTICs, as shown by down-regulation of an epithelial marker (E-cadherin) and up-regulation of mesenchymal markers (N-cadherin and vimentin) as well as an EMT regulator (Twist) (Supplementary Fig. S2E). Furthermore, Seahorse analysis and MTT assay demonstrated a more glycolytic state as well as chemotherapy resistance to cisplatin treatment in isolated BTICs (31-32) (Supplementary Fig. S2F and G). Altogether, these results provide a proof of concept that typical features of BTICs could be recapitulated upon hypoxia and HIF-1 $\alpha$  overexpression.

### **Direct regulation of TET by hypoxia is critical for regulation of BTICs**

Next we investigated whether certain epigenetic regulators might be required for the hypoxia effect contributing to acquisition of BTIC properties. We found that hypoxia treatment significantly increased the expression of TET1 and TET3 in

primary cultures as well as breast cancer cell lines (Supplementary Fig. S3A-D), whereas no significant changes in TET2 expression were observed upon hypoxia. In support of these observations, overexpression of HIF-1 $\alpha$  consistently increased the expression of both TET1 and TET3 in cancer cell lines (Supplementary Fig. S3E and F). To investigate the molecular mechanisms by which hypoxia regulates the expression of TET1 and TET3, we analyzed TET1/TET3 promoter sequences and identified putative HIF-1 $\alpha$  binding sites (33) (Fig. 2A). Luciferase reporter assays further showed increases in the promoter activity of TET1 and TET3 as a response to hypoxia as well as upon overexpression of HIF-1 $\alpha$ . Directed mutagenesis of the putative HIF-1 $\alpha$  binding site in TET1/TET3 promoters abolished luciferase activity under hypoxic conditions as well as upon ectopic expression of HIF-1 $\alpha$  (Fig. 2B). qChIP analysis confirmed that HIF-1 $\alpha$  bound to both TET1 and TET3 gene promoters containing HRE in hypoxic cells, whereas no significant HIF-1 $\alpha$  bindings on a distal promoter without HRE were observed (Fig. 2C). Increased binding of HIF-1 $\alpha$  to the promoter regions of TET1 and TET3 genes was readily observed in breast cancer cell lines, MCF7 or MDA-MB-231 upon overexpression of HIF-1 $\alpha$  (Supplementary Fig. S4A and B). Furthermore, knockdown of HIF1 $\alpha$  reduced the hypoxia effect on activation of both TET1 and TET3 genes in breast cancer cell lines (data not shown). Taken together, these results indicate that HIF-1 $\alpha$  directly regulates the transcription

of TET1 and TET3 as a response to hypoxia.

The significant increase of TET1 and TET3 expression in isolated BTICs suggested a role for TET proteins in hypoxia induced BTIC properties (Supplementary Fig. S3G and H). For further investigation, we performed shRNA mediated gene knock-down experiments for TET1 and TET3. Down-regulation of either TET1 or TET3 reduced the up-regulation of stem cell markers as a result of hypoxia (Supplementary Fig. S5A and B), whereas silence of TET1 or TET3 did not affect HIF-1 activity, as shown by HIF-1 $\alpha$  binding on the *VEGF* promoter in hypoxic cells (Supplementary Fig. S5C and D). Likewise, knockdown of TET in isolated BTICs reduced BTIC properties including CD44<sup>+</sup>/CD24<sup>-</sup> and ALDH<sup>+</sup> populations as well as EMT process (Fig. 3A-C). Mammosphere-forming assays further showed compromised self-renewal in isolated BTICs when TET genes were silenced (Fig. 3E). Moreover, co-silencing of TET1 and TET3 sensitized isolated BTICs to paclitaxel, a widely used chemotherapy drug for the treatment of breast cancer (Fig. 3F). To confirm the role of TET proteins *in vivo*, we performed subcutaneous and orthotopic tumor formation assays. The subcutaneous xenograft study showed that HIF-1 $\alpha$  overexpressing cells and isolated BTICs led to the formation of larger tumors as compared to control cells. Inversely, knockdown of TET1 and TET3 expression in isolated BTICs reduced tumor growth

(Fig. 3G, Supplementary Fig. S6A and B). To further determine the role of TET1/3 in tumor initiating capability, we performed limited dilution experiments. As expected, the results indicated a more malignant phenotype for HIF-1 $\alpha$  overexpressing cells as well as isolated BTICs. Down-regulation of TET1 and TET3 resulted in decreased tumorigenicity in isolated BTICs (Fig. 3H and Fig. S6C). Serial transplantation, a gold standard for defining cancer stem cell characteristics *in vivo* (34), demonstrated that isolated BTICs led to secondary tumor formation. Inversely, knockdown of TET1/TET3 impaired secondary tumor formation (Fig. 3I and Supplementary Fig. S6D). Together, these results demonstrate that TET proteins play a critical role in the acquisition of BTIC characteristics upon hypoxia.

### **TET1, TET3 and 5hmC levels are correlated with tumor hypoxia, tumor malignancy, and poor prognosis of patients**

To evaluate the clinical significance of the aforementioned results, we analyzed the levels of three members of the TET family in 165 cases of patients with breast tumors. As expected, we found that the levels of 5hmC, TET1 and TET3 were significantly associated with tumor hypoxia (Fig. 4A, Supplementary Fig. S7 and Supplementary Tables S1), as indicated by staining for HIF1 $\alpha$ , whereas no significant correlation with hypoxia for TET2 expression was observed (data not shown). The fact that

hypoxia is tightly associated with high grade breast tumor and poor prognosis of patients with breast cancer prompted us to investigate whether TET1, TET3 and 5hmC levels correlate with malignant phenotypes of breast tumor. Our results indicated that TET1 and TET3 were highly expressed in both high-grade (comedo-type) *ductal carcinoma in situ* (DCIS) ( $p < 0.001$  and  $p < 0.001$ , respectively, Fig. 4A and B) and grade 3 *invasive ductal carcinoma* (IDC) samples ( $p < 0.05$  and  $p < 0.05$ , respectively, Fig. 4A and B). In line with TET1/3 expression patterns, high levels of 5hmC were observed in high grade DCIS and IDC ( $p < 0.001$  and  $p < 0.05$ , respectively, Fig. 4A and B). Histological analysis demonstrated the presence of TET1 and TET3 as well as 5hmC in the invasive front of breast tumors, an infiltrative phenotype correlated with tumor malignancy (35) (Fig. 4C). Furthermore, the levels of TET1, TET3 and 5hmC all showed a significant association with poor patient overall survival (OS) and disease-free survival (DFS) (Fig. 4D and E). Collectively, these results indicate that TET1, TET3 and 5hmC levels correlate with tumor hypoxia, tumor aggressiveness and poor prognosis of patients with breast cancer.

**Genome-wide changes in DNA hydroxymethylation resulting from hypoxia is associated with activation of TNF $\alpha$ -p38-MAPK signaling**

TET1 and TET3 proteins possess methylcytosine hydroxylase activity to mediate

the conversion of 5mC to 5hmC (19). Accordingly, we next asked whether 5hmC levels contribute to the hypoxia-induced aggressiveness of breast cancer. Dot blot analysis indicated a global increase in the levels of 5hmC (Fig. 5A). Immunoprecipitation with antibodies against 5hmC (hMe-DIP) followed by deep sequencing demonstrated increased 5hmC levels over broad chromatin domains, most notably in gene-rich regions (Fig. 5B). These domains bore striking similarity to chromatin found in the ‘active’ compartment of the genome as determined by Hi-C, a method that uses spatial proximity ligation to measure the conformation of the genome (27). Principal Component Analysis (PCA) of published Hi-C data (36) compared to our own ChIP data suggested a correlation between 5hmC and the spatial segregation of open and closed chromatin (Fig. 5B and C), with large increases in 5hmC levels found exclusively in the active compartment (positive PC1 values). Together, these results indicate that hypoxia results in genome-wide changes in DNA hydroxymethylation.

We next identified 1794 gene promoters, in which hypoxia led to an increase in 5hmC levels ( $\geq 1.5$  fold). In agreement with a previous report (37), Gene Ontology (GO) highlighted biological processes related to the plasma membrane, development, and cell adhesion (Fig. 5D and E). Comparison of ChIP-seq and RNA-seq data led to

the identification of 389 commonly regulated genes. Interestingly, GO analysis for these 389 genes highlighted TNF signaling as a prime candidate for regulation by hypoxia (Fig. 5F). hMe-DIP with two sets of primers against different genomic regions of the TNF $\alpha$  gene consistently showed an increased 5hmC level in these regions as well as RNA polII binding at the transcription start site (TSS) in either MCF7 or MDA-MB-231 as a response to hypoxia (Fig. 5G and H) as well as in HIF-1 $\alpha$  overexpressing cells and isolated BTICs (Supplementary Fig. S8A and B). However, there were no significant changes in 5hmC levels as well as TET1/3 protein bindings on the remote genome region and unrelated gene promoter (*HSP90* gene) in hypoxic cells, HIF-1 $\alpha$  overexpressing cells and isolated BTICs (Supplementary Fig. S8C-F). The qChIP results showed no significant HIF-1 $\alpha$  binding on different genomic regions of the TNF $\alpha$  gene, suggesting that hypoxia might not regulate TNF $\alpha$  expression directly (Supplementary Fig. S8G). To exclude the possibility that this gene-specific change in 5hmC levels is a general effect that might be induced by some other stress, we examined the 5hmC levels in serum-starved cells. Upon starvation, there were no significant changes in 5hmC level on TNF $\alpha$  gene, indicating a specific role for hypoxia in regulating gene-specific 5hmC changes (Supplementary Fig. S9A). In addition, in line with aforementioned results, hypoxia resulted in the upregulation of TNF $\alpha$  in both primary cultures and cancer cell lines (Fig. 6A-D), whereas TNF $\alpha$

gene expression was not changed in serum-starved cells (Supplementary Fig. S9B). Increased levels of TNF $\alpha$  were observed in HIF-1 $\alpha$  overexpressing cells and isolated BTICs (Fig. 6E-H). Together, these results indicate that gene-specific changes of 5hmC were associated with the expression of TNF $\alpha$  gene. Since TNF $\alpha$  activation has been described to induce p38-MAPK signaling, an important regulator in cancer progression (38-39), we next examined the role of hypoxia in this context. Western blot analysis demonstrated increased phosphorylation of p38-MAPK in response to hypoxia (Fig. 6B and D) as well as in HIF-1 $\alpha$  overexpressing cells and isolated BTICs (Fig. 6F and H). In addition, ELISA assays demonstrated elevated levels of TNF $\alpha$  in hypoxic cells, HIF-1 $\alpha$  overexpressing cells and isolated BTICs compared to control cells (Fig. 6I-K). These results suggest that hypoxia mediated DNA hydroxymethylation defines a layer of epigenetic regulation for the activation of TNF $\alpha$ -p38-MAPK signaling.

### **TET proteins are essential for hypoxia-induced TNF $\alpha$ -p38-MAPK signaling**

To further investigate whether TET proteins mechanistically mediate the activation of TNF $\alpha$ -p38-MAPK signaling in response to hypoxia, we knocked down either TET1 or TET3 expression in breast cancer cell lines. As expected, TNF $\alpha$  expression and phosphorylation of p38-MAPK were suppressed upon knockdown of either TET1

or TET3 in hypoxic condition (Supplementary Fig. S10A-D). Likewise, silencing TET1 or TET3 repressed the TNF $\alpha$ -p38-MAPK signaling cascade in isolated BTICs (Supplementary Fig. S10E-H). hMe-DIP analysis further indicated an attenuation in the levels of 5hmC in the promoter region of TNF $\alpha$  upon TET knockdown as a response to hypoxia (Supplementary Fig. S11A and B). Consistently, silence of TET reduced 5hmC levels in HIF-1 $\alpha$  overexpressing cells and isolated BTICs (Supplementary Fig. S11C-F). To more stringently assess the role of TET proteins in hypoxia-induced TNF $\alpha$ -p38-MAPK signaling, the rescue experiment was performed using either wild type or inactive mutant forms of TET1 and TET3. Re-expressing wild type of TET1, but not inactive TET1 mutant, was capable of restoring the hypoxia effect on induction of 5hmC in TET1 knockdown cells (Supplementary Fig. S12A and B). Likewise, the induction of 5hmC by hypoxia was restored by re-expression of the wild type of TET3, but not the inactive TET3 mutant, in TET3 deficient cells (Supplementary Fig. S12C and D). Furthermore, as shown by western blot analysis, re-expression of either wild type of TET1 or TET3 was capable of restoring the activation of TNF $\alpha$ -p38-MAPK signaling, whereas inactive TET mutants were unable to rescue this phenomenon (Supplementary Fig. S13A-D). These results indicate an essential role for TET1 and TET3 in hypoxia-induced TNF $\alpha$ -p38-MAPK signaling.

### **TET1 and TET3 coordinately mediate the activation of TNF $\alpha$ -p38-MAPK signaling in response to hypoxia**

Given that single knockdown of either TET1 or TET3 resulted in similar effects, we next asked whether they could function coordinately in response to hypoxia. TET1 co-immunoprecipitation experiments demonstrated the physical interaction of TET1 and TET3 proteins in hypoxic samples (Supplementary Fig. S14A and B). Inverse co-IP experiments, using an anti-TET3 antibody, further confirmed an interaction between TET3 and TET1 (Supplementary Fig. S14C and D). Likewise, physical interactions between TET1 and TET3 were also observed in isolated BTICs (Supplementary Fig. S14E and F). To examine whether TET1-TET3 complexes occupy the TNF $\alpha$  gene promoter, we performed serial ChIP assays. Indeed, co-occupancy of TET1 and TET3 was observed in breast cancer cell lines as a response to hypoxia (Supplementary Fig. S15A-D). Decreased binding of the protein complex to the TNF $\alpha$  promoter was observed upon individual knockdown of either TET1 or TET3 in HIF-1 $\alpha$  overexpressing cells and isolated BTICs. (Supplementary Fig. S15E-L). Collectively, these results indicate that TET1 and TET3 function cooperatively to regulate TNF $\alpha$ -p38-MAPK signaling upon hypoxia.

### **TNF $\alpha$ -p38-MAPK signaling is essential in maintaining BTIC properties**

The TNF- $\alpha$  signaling pathway contributes to the acquisition of BTIC properties (33,40). Likewise, activation of p38-MAPK has been shown to correlate with increased tumor malignancy and poor prognosis of cancer patients (41-43). Therefore, we next attempted to block hypoxia-elicited responses by disrupting this signaling pathway. We found that BTIC phenotypes were suppressed upon treatment with TNF $\alpha$ -neutralizing antibodies (Fig. 7A-C). Similarly, chemical inhibition of p38-MAPK led to compromised BTIC phenotypes in isolated BTICs (Supplementary Fig. S16A-C) and resulted in increased cell death upon paclitaxel treatment (Supplementary Fig. S16D). In order to further confirm these results, we performed TNF $\alpha$  knockdown experiments in isolated BTICs (Fig. 7D). Knockdown of TNF $\alpha$  resulted in reduced phosphorylation of p38-MAPK (Fig. 7G). BTIC properties including CD44<sup>+</sup>/CD24<sup>-</sup> populations, ALDH<sup>+</sup> population, EMT process, as well as mammosphere forming ability, were decreased when TNF $\alpha$  was silenced (Fig. 7E-H). Moreover, down-regulation of TNF $\alpha$  sensitized isolated BTICs to paclitaxel treatment (Fig. 7I). Noticeably, xenograft studies showed that TNF $\alpha$  knockdown hampered tumor initiating capabilities *in vivo*, suggesting a critical role for TNF $\alpha$  in hypoxia-enhanced tumorigenicity (Fig. 7J). Next, we asked whether inhibition of p38 MAPK signaling might be sufficient for attenuating tumor forming potential *in vivo*.

To this end, cells were injected into mice and then animals were treated with p38-MAPK inhibitor for 3 weeks. Our results demonstrated decreased tumor formation ability, but not decreased tumor growth, upon inhibition of p38-MAPK in both subcutaneous and orthotopic tumor formation assays (Supplementary Fig. S16E and F and data not shown). To ensure the hierarchy with respect to the TNF $\alpha$ -p38-MAPK cascade in isolated BTICs, we examined the expression of their downstream targets in this context (44). We found that the expression of selected targets including *IL-1 $\beta$* , *IL-11*, *MMP3*, *MMP9*, *GFBP2*, *PTGS2* and *TGM2* was upregulated in isolated BTICs. Treatment of TNF $\alpha$ -neutralizing antibodies and p38-MAPK inhibitor reduced the expression level for all of these genes (Supplementary Fig. S17A and B). In addition, these genes were regulated by hypoxia, whereas knocking down either TET1 or TET3 abolished this effect (Supplementary Fig. S17C). These data collectively suggest that the TNF $\alpha$ -p38-MAPK signaling cascade, activated by TET proteins in response to hypoxia, plays a vital role in maintaining BTIC capabilities.

## **Discussion**

In the present study, we demonstrated a novel pathway by which hypoxia promotes tumor malignancy through TET-mediated activation of TNF $\alpha$ -p38-MAPK signaling.

Hypoxia was found to regulate TET1 and TET3 expression through HIF-1 $\alpha$ , which led to global changes in DNA hydroxymethylation, associated with tumor malignancy. Upon hypoxia, TET proteins functioned coordinately to activate the TNF $\alpha$ -p38-MAPK signaling pathway, resulting in BTIC properties. Recent findings suggest that hypoxia contributes to the formation of a tumor initiating cells niche within the tumor where hypoxia influences the behavior of TICs as well as their tumorigenic capacity (45). Consistent with this, as a proof-of-principle, our results demonstrated that hypoxia recapitulated such phenotypes in breast cancer, suggesting hypoxia as a critical factor driving tumor malignancy. Epigenetic alterations occurring in breast cancer cells have been suggested to render heterogeneity to breast tumors, resulting in BTIC phenotypes and tumor malignancy (46). Together with our findings, it indicates that the function of TET proteins is required for hypoxia induced BTICs, therefore providing a direct link with tumor malignancy for hypoxia-induced deregulation of DNA methylation. Despite this, the role of TET proteins in cancer progression has been debated. Our findings presented here are linked with an oncogenic role for TET proteins; this is consistent with previous reports demonstrating that TET proteins are associated with prognostic epigenetic signature and the regulation for a set of important oncogenic targets (47-48). Reduced 5hmC level was found in some types of cancer as compared to corresponding normal tissue

(49), however the correlation of 5hmC level as well as the related enzyme- TET proteins with tumor grading in breast cancer has not been thoroughly dissected. Our findings extensively demonstrated that 5hmC as well as TET1 and TET3 were expressed at a high level in high grade DCIS, and a gradient expression for all of these three factors in IDC was also noted, which is consistent with the notion that a poorly differentiated breast tumor displays a higher content of breast tumor initiating cells than a well differentiated one (10). The tumor suppressor role has been proposed for TET proteins (50). However, the central role of TET proteins in mediating hypoxia-induced tumor malignancy has suggested that the function of TET is redefined by the tumor microenvironment compartment, which, in turn, indicates a complex interaction between the cancer epigenome and tumor microenvironment. It would be of interest in the future, to study the significance of different oncogenic contexts in determining pathological function of TET proteins that will help us better understand the epigenetic regulation during cancer progression.

Re-modeling DNA methylation profile by hypoxia has been demonstrated in certain cell types including normal and cancer cells (51-52). Our results showed that hypoxia led to global changes in 5hmC level through direct regulation of TET1 and TET3, suggesting a novel mechanism by which hypoxia contributes to dynamic

change of DNA methylation profile during cancer progression. Increased DNA hydroxymethylation was evident at various pluripotent loci such as *Oct4* and *Nanog* during pluripotent reprogramming (22). We readily observed the occupancy for TET proteins at pluripotent loci upon hypoxia (Supplementary Fig. S18 A and B, Supplementary Fig. S19 A and B), whereas the changes of DNA hydroxymethylation were not significantly correlated with this phenomenon (Supplementary Fig. S18 C and D, Supplementary Fig. S19 C and D), suggesting an intricate mechanism for hypoxia in regulating pluripotency genes. Moreover, our results showed a coordinate function of TET proteins, suggesting the importance of interacting partners in the regulation of the biological function of TET proteins. Since hypoxia targets different histone modifiers that may orchestrate with DNA methylation, contributing to tumor progression (16), it will be interesting to investigate the synergistic function of TET proteins with different epigenetic regulators in regulating the cancer epigenome and tumor malignancy.

Previous studies showed that tumor necrosis factor- $\alpha$  (TNF- $\alpha$ ) stimulates many signaling pathways, resulting in the activation of multiple signaling cascades that contribute to cancer progression as well as BTICs characteristics (33,40). Likewise, p38-MAPK signaling, a downstream target of TNF- $\alpha$ , has been suggested as an

important regulator in cancer progression and tumor initiation (41,53). Our findings unveil, for the first time, a direct mechanistic link between hypoxia-TET proteins and the regulation of the cancer epigenome for the activation of the TNF $\alpha$ -p38-MAPK pathway in regulating BTICs. The results demonstrated that certain downstream targets of TNF $\alpha$ -p38-MAPK signaling known to contribute to cancer stemness, including *IL-1 $\beta$* , *MMP3*, *MMP9*, *GFBP2* and *PTGS2*, were enriched in BTICs and regulated by hypoxia-TET-TNF $\alpha$ -p38-MAPK signaling axis have suggested a potential mechanism for this signaling in regulating stemness of breast cancer (Supplementary Fig. S17). However, the precise mechanism needs to be delineated in future studies.

Finally, recent reports describing the influence of hypoxia on regulation of BTICs have suggested tumor hypoxia as an attractive target for therapeutic intervention (12). Acquisition of epigenetic alterations gives tumor cells the ability to expand and adapt to the changing microenvironment and clinical treatment, suggesting a therapeutic strategy targeting epigenetic mechanisms and related downstream signaling pathways. Herein our results suggest a novel mechanism of epigenetic regulation in cancer cells as a response to hypoxia and additionally highlight TET1 and TET3 as novel prognostic biomarkers for breast cancer. Most importantly, targeting the

hypoxia-TET-TNF $\alpha$ -p38-MAPK signaling axis indicates a promising inhibitory effect on tumor malignancy. Thus, our results shed new light on the role of hypoxia in regulating the cancer epigenome leading to breast cancer malignancy, providing novel strategies for the future development of therapeutic strategies.

### **Grant Support**

This work was supported by grants from the G. Harold and Leila Y. Mathers Charitable Foundation and The Leona M. and Harry B. Helmsley Charitable Trust.

### **Acknowledgements**

We greatly appreciate Drs. Geoffrey Wahl and Kou-Juey Wu for comments on this manuscript and insightful discussions. We thank Dr. Kou-Juey Wu for the gifts of the pGL reporter and  $\beta$ -gal plasmid. We are grateful to Drs. Sven Heinz and Manching Ku of the Next Generation Sequencing Core, Salk Institute for Biological Studies for technical assistance.

## References:

1. Di Cosimo S, Baselga J. Management of breast cancer with targeted agents: importance of heterogeneity. [corrected]. *Nat Rev Clin Oncol* 2010;7(3):139-47.
2. Reya T, Morrison SJ, Clarke MF, Weissman IL. Stem cells, cancer, and cancer stem cells. *Nature* 2001;414(6859):105-11.
3. Singh SK, Clarke ID, Terasaki M, Bonn VE, Hawkins C, Squire J, et al. Identification of a cancer stem cell in human brain tumors. *Cancer Res* 2003;63(18):5821-8.
4. Prince ME, Sivanandan R, Kaczorowski A, Wolf GT, Kaplan MJ, Dalerba P, et al. Identification of a subpopulation of cells with cancer stem cell properties in head and neck squamous cell carcinoma. *Proc Natl Acad Sci U S A* 2007;104(3):973-8.
5. Bertolini G, Roz L, Perego P, Tortoreto M, Fontanella E, Gatti L, et al. Highly tumorigenic lung cancer CD133+ cells display stem-like features and are spared by cisplatin treatment. *Proc Natl Acad Sci U S A* 2009;106(38):16281-6.
6. Ponti D, Costa A, Zaffaroni N, Pratesi G, Petrangolini G, Coradini D, et al. Isolation and in vitro propagation of tumorigenic breast cancer cells with stem/progenitor cell properties. *Cancer Res* 2005;65(13):5506-11.
7. Al-Hajj M, Wicha MS, Benito-Hernandez A, Morrison SJ, Clarke MF. Prospective identification of tumorigenic breast cancer cells. *Proc Natl Acad Sci U S A* 2003;100(7):3983-8.
8. Ginestier C, Hur MH, Charafe-Jauffret E, Monville F, Dutcher J, Brown M, et al. ALDH1 is a marker of normal and malignant human mammary stem cells and a predictor of poor clinical outcome. *Cell Stem Cell* 2007;1(5):555-67.
9. Visvader JE, Lindeman GJ. Cancer stem cells in solid tumours: accumulating evidence and unresolved questions. *Nat Rev Cancer* 2008;8(10):755-68.
10. Pece S, Tosoni D, Confalonieri S, Mazzarol G, Vecchi M, Ronzoni S, et al. Biological and molecular heterogeneity of breast cancers correlates with their cancer stem cell content. *Cell* 2010;140(1):62-73.
11. Stingl J, Caldas C. Molecular heterogeneity of breast carcinomas and the cancer stem cell hypothesis. *Nat Rev Cancer* 2007;7(10):791-9.
12. Semenza GL. Molecular mechanisms mediating metastasis of hypoxic breast cancer cells. *Trends Mol Med* 2012;18(9):534-43.
13. Dales JP, Garcia S, Meunier-Carpentier S, Andrac-Meyer L, Haddad O, Lavaut MN, et al. Overexpression of hypoxia-inducible factor HIF-1alpha

- predicts early relapse in breast cancer: retrospective study in a series of 745 patients. *Int J Cancer* 2005;116(5):734-9.
14. Keith B, Simon MC. Hypoxia-inducible factors, stem cells, and cancer. *Cell* 2007;129(3):465-72.
  15. Borovski T, De Sousa EMF, Vermeulen L, Medema JP. Cancer stem cell niche: the place to be. *Cancer Res* 2011;71(3):634-9.
  16. Wu MZ, Tsai YP, Yang MH, Huang CH, Chang SY, Chang CC, et al. Interplay between HDAC3 and WDR5 is essential for hypoxia-induced epithelial-mesenchymal transition. *Mol Cell* 2011;43(5):811-22.
  17. Taddei ML, Giannoni E, Comito G, Chiarugi P. Microenvironment and tumor cell plasticity: an easy way out. *Cancer Lett* 2013;341(1):80-96.
  18. Dawson MA, Kouzarides T. Cancer epigenetics: from mechanism to therapy. *Cell* 2012;150(1):12-27.
  19. Ito S, Shen L, Dai Q, Wu SC, Collins LB, Swenberg JA, et al. Tet proteins can convert 5-methylcytosine to 5-formylcytosine and 5-carboxylcytosine. *Science* 2011;333(6047):1300-3.
  20. Wu H, Zhang Y. Mechanisms and functions of Tet protein-mediated 5-methylcytosine oxidation. *Genes Dev* 2011;25(23):2436-52.
  21. Ko M, Huang Y, Jankowska AM, Pape UJ, Tahiliani M, Bandukwala HS, et al. Impaired hydroxylation of 5-methylcytosine in myeloid cancers with mutant TET2. *Nature* 2010;468(7325):839-43.
  22. Gu TP, Guo F, Yang H, Wu HP, Xu GF, Liu W, et al. The role of Tet3 DNA dioxygenase in epigenetic reprogramming by oocytes. *Nature* 2011;477(7366):606-10.
  23. Charafe-Jauffret E, Tarpin C, Bardou VJ, Bertucci F, Ginestier C, Braud AC, et al. Immunophenotypic analysis of inflammatory breast cancers: identification of an 'inflammatory signature'. *J Pathol* 2004;202(3):265-73.
  24. Langmead B, Salzberg SL. Fast gapped-read alignment with Bowtie 2. *Nat Methods* 2012;9(4):357-9.
  25. Heinz S, Benner C, Spann N, Bertolino E, Lin YC, Laslo P, et al. Simple combinations of lineage-determining transcription factors prime cis-regulatory elements required for macrophage and B cell identities. *Mol Cell* 2010;38(4):576-89.
  26. Robinson MD, McCarthy DJ, Smyth GK. edgeR: a Bioconductor package for differential expression analysis of digital gene expression data. *Bioinformatics* 2010;26(1):139-40.
  27. Lin YC, Benner C, Mansson R, Heinz S, Miyazaki K, Miyazaki M, et al. Global changes in the nuclear positioning of genes and intra- and interdomain

- genomic interactions that orchestrate B cell fate. *Nat Immunol* 2012;13(12):1196-204.
28. Yang MH, Hsu DS, Wang HW, Wang HJ, Lan HY, Yang WH, et al. Bmi1 is essential in Twist1-induced epithelial-mesenchymal transition. *Nat Cell Biol* 2010;12(10):982-92.
  29. Ben-Porath I, Thomson MW, Carey VJ, Ge R, Bell GW, Regev A, et al. An embryonic stem cell-like gene expression signature in poorly differentiated aggressive human tumors. *Nat Genet* 2008;40(5):499-507.
  30. Mani SA, Guo W, Liao MJ, Eaton EN, Ayyanan A, Zhou AY, et al. The epithelial-mesenchymal transition generates cells with properties of stem cells. *Cell* 2008;133(4):704-15.
  31. Feng W, Gentles A, Nair RV, Huang M, Lin Y, Lee CY, et al. Targeting Unique Metabolic Properties of Breast Tumor Initiating Cells. *Stem Cells* 2014.
  32. Shafee N, Smith CR, Wei S, Kim Y, Mills GB, Hortobagyi GN, et al. Cancer stem cells contribute to cisplatin resistance in Brca1/p53-mediated mouse mammary tumors. *Cancer Res* 2008;68(9):3243-50.
  33. Asiedu MK, Ingle JN, Behrens MD, Radisky DC, Knutson KL. TGFbeta/TNF(alpha)-mediated epithelial-mesenchymal transition generates breast cancer stem cells with a claudin-low phenotype. *Cancer Res* 2011;71(13):4707-19.
  34. Beck B, Blanpain C. Unravelling cancer stem cell potential. *Nat Rev Cancer* 2013;13(10):727-38.
  35. Takasaki T, Akiba S, Sagara Y, Yoshida H. Histological and biological characteristics of microinvasion in mammary carcinomas  $\leq 2$  cm in diameter. *Pathol Int* 1998;48(10):800-5.
  36. Kalhor R, Tjong H, Jayathilaka N, Alber F, Chen L. Genome architectures revealed by tethered chromosome conformation capture and population-based modeling. *Nat Biotechnol* 2011;30(1):90-8.
  37. Tsuchihara K, Suzuki Y, Wakaguri H, Irie T, Tanimoto K, Hashimoto S, et al. Massive transcriptional start site analysis of human genes in hypoxia cells. *Nucleic Acids Res* 2009;37(7):2249-63.
  38. Zarubin T, Han J. Activation and signaling of the p38 MAP kinase pathway. *Cell Res* 2005;15(1):11-8.
  39. Li YP, Chen Y, John J, Moylan J, Jin B, Mann DL, et al. TNF-alpha acts via p38 MAPK to stimulate expression of the ubiquitin ligase atrogin1/MAFbx in skeletal muscle. *FASEB J* 2005;19(3):362-70.
  40. Bhat-Nakshatri P, Appaiah H, Ballas C, Pick-Franke P, Goulet R, Jr., Badve S, et al. SLUG/SNAI2 and tumor necrosis factor generate breast cells with

- CD44+/CD24- phenotype. *BMC Cancer* 2010;10:411.
41. Hennessy BT, Gonzalez-Angulo AM, Stemke-Hale K, Gilcrease MZ, Krishnamurthy S, Lee JS, et al. Characterization of a naturally occurring breast cancer subset enriched in epithelial-to-mesenchymal transition and stem cell characteristics. *Cancer Res* 2009;69(10):4116-24.
  42. Esteva FJ, Sahin AA, Smith TL, Yang Y, Pusztai L, Nahta R, et al. Prognostic significance of phosphorylated P38 mitogen-activated protein kinase and HER-2 expression in lymph node-positive breast carcinoma. *Cancer* 2004;100(3):499-506.
  43. Whyte J, Bergin O, Bianchi A, McNally S, Martin F. Key signalling nodes in mammary gland development and cancer. Mitogen-activated protein kinase signalling in experimental models of breast cancer progression and in mammary gland development. *Breast Cancer Res* 2009;11(5):209.
  44. Zer C, Sachs G, Shin JM. Identification of genomic targets downstream of p38 mitogen-activated protein kinase pathway mediating tumor necrosis factor-alpha signaling. *Physiol Genomics* 2007;31(2):343-51.
  45. Mohyeldin A, Garzon-Muvdi T, Quinones-Hinojosa A. Oxygen in stem cell biology: a critical component of the stem cell niche. *Cell Stem Cell* 2010;7(2):150-61.
  46. Meacham CE, Morrison SJ. Tumour heterogeneity and cancer cell plasticity. *Nature* 2013;501(7467):328-37.
  47. Zhuang J, Jones A, Lee SH, Ng E, Fiegl H, Zikan M, et al. The dynamics and prognostic potential of DNA methylation changes at stem cell gene loci in women's cancer. *PLoS Genet* 2012;8(2):e1002517.
  48. Huang H, Jiang X, Li Z, Li Y, Song CX, He C, et al. TET1 plays an essential oncogenic role in MLL-rearranged leukemia. *Proc Natl Acad Sci U S A* 2013;110(29):11994-9.
  49. Lian CG, Xu Y, Ceol C, Wu F, Larson A, Dresser K, et al. Loss of 5-hydroxymethylcytosine is an epigenetic hallmark of melanoma. *Cell* 2012;150(6):1135-46.
  50. Hsu CH, Peng KL, Kang ML, Chen YR, Yang YC, Tsai CH, et al. TET1 suppresses cancer invasion by activating the tissue inhibitors of metalloproteinases. *Cell Rep* 2012;2(3):568-79.
  51. Shahrzad S, Bertrand K, Minhas K, Coomber BL. Induction of DNA hypomethylation by tumor hypoxia. *Epigenetics* 2007;2(2):119-25.
  52. Liu Q, Liu L, Zhao Y, Zhang J, Wang D, Chen J, et al. Hypoxia induces genomic DNA demethylation through the activation of HIF-1alpha and transcriptional upregulation of MAT2A in hepatoma cells. *Mol Cancer Ther*

2011;10(6):1113-23.

53. Oeztuerk-Winder F, Ventura JJ. The many faces of p38 mitogen-activated protein kinase in progenitor/stem cell differentiation. *Biochem J* 2012;445(1):1-10.

## Figure Legends

### Figure 1 Hypoxia promotes stem cell-like features in breast cancer cells.

A, Hypoxia increases the subpopulation of cells harboring CD44<sup>+</sup>/CD 24<sup>-</sup> phenotype in primary breast cancer cells. Left: representative FACS analysis for cells expressing CD44<sup>+</sup>/CD 24<sup>-</sup> markers in hypoxia (H) vs. normoxia (N). Right: quantitative results of FACS analysis showing an increase of the percentage of cells with CD44<sup>+</sup>/CD 24<sup>-</sup> markers under hypoxia treatment. B, Hypoxia increases the population of ALDEFLUOR-positive (ALDH<sup>+</sup>) cells. C, RT-qPCR analysis of stemness related genes (Oct4, Sox2 and Nanog) in hypoxic primary cells vs. normoxic primary cells. D and E, hypoxia treatment increases the population of cells expressing CD44<sup>+</sup>/CD 24<sup>-</sup> or ALDH1 activity in breast cancer cell lines (MCF7 and MDA-MB-231). F, Gene expression analysis for stemness related genes in cancer cells treated with hypoxia. G, Spheroid formation assay showed an increased cellular ability for sphere formation in primary cells and cancer cell lines upon hypoxia. Top: representative images for sphere of hypoxic cells. Bottom: quantitative results of spheroid assay in hypoxia vs. normoxia. The scale bars represent 50  $\mu$ m. All the data are presented as means  $\pm$  SD ( $n=3$ ). Asterisk indicates  $P < 0.05$ , compared with controls.

### Figure 2 Hypoxia regulates TET1 and TET3 expression via HIF-1 $\alpha$ .

A, Schematic representation for the hypoxia response element in TET1 or TET3 gene promoter and reporter constructs used in gene promoter activity assays. B, Left: the fold change of TET1 gene promoter activity under normoxia or hypoxia with or without transfection of HIF-1 $\alpha$ . Right: the fold change of TET3 gene promoter activity in the same conditions as indicated in the left panel. Asterisk indicates  $P < 0.05$ , compared with normoxic cells transfected with control vector. C, ChIP assay for HIF-1 $\alpha$  binding on TET1 (left panel) and TET3 (middle panel) gene promoter in hypoxic cancer cells. Primer-targeted regions in ChIP assay are noted, as indicated. Proximal region (P1) in either TET1 or TET3 gene promoter was used as a negative control. VEGF gene promoter (right panel) was used a positive control for HIF-1 $\alpha$  binding upon hypoxia. N: normoxia H: hypoxia. All the data are presented as means  $\pm$  SD ( $n=3$ ). Asterisk indicates  $P < 0.05$ , compared with controls.

**Figure 3 TET1 and TET3 are required for hypoxia-enhanced tumor malignancy.**

A, shRNA-mediated gene silencing of TET1 and/or TET3 represses expression of stemness related genes in isolated BTICs derived from HIF-1 $\alpha$  overexpressing cells. Top: the changes in the mRNA level of stemness genes in isolated BTICs undergoing single knockdown of either TET1 or TET3, or co-silencing of TET1 and TET3. Bottom: the protein level of TET1 and TET3 in different cells by western blot. Two

shRNA for either TET1 or TET3 were used, as indicated. EGFP shRNA was used as a negative control. B, Decreased subpopulation of cells expressing CD44<sup>+</sup>/CD24<sup>-</sup> phenotype in TET gene knockdown cells. C, Knocking down TET1 and/or TET3 expression reduces the population of ALDEFLUOR-positive (ALDH<sup>+</sup>) cells in isolated BTICs. Diethylaminobenzaldehyde (DEAB), a specific inhibitor of ALDH1, was used to define the ALDEFLUOR-positive cell population. D, Western blot analysis of an epithelial marker (E-cadherin), mesenchymal markers (*N*-cadherin and vimentin) and EMT regulator (Twist) showing a reduced EMT process in isolated BTICs stably expressing TET1, TET3 or TET1/3 shRNAs. E, The quantification of spheroid formation assay for isolated BTICs stably expressing shRNA of either TET1 or TET3, or both. Three rounds of spheroid formation assay were performed, as indicated. F, Decreased drug resistance to paclitaxel treatment in isolated BTICs undergoing co-silencing of TET1 and TET3. G, Tumor growth analysis showed down-regulation of TET reduced hypoxia-enhanced tumor formation ability. HIF-1 $\alpha$  overexpressing cells, isolated BTICs, TET1/3 co-silencing BTICs and control cells were xenografted on mice. The cells were injected at 1X10<sup>5</sup> cellular dose. H, The statistical results of incidence for tumor formation in mice subcutaneously injected with control, HIF-1 $\alpha$  overexpressing cells, isolated BTICs and TET1/3 co-silencing BTICs in serial dilution of cellular doses. Asterisk indicates  $P < 0.05$  comparing

between isolated BTICs and control cells. Double asterisk indicates  $P < 0.05$  comparing between TET1/3 co-silencing BTICs and isolated BTICs. I, Co-silence of TET1/3 decreased secondary tumor formation ability of isolated BTICs. Left: *in vivo* images for secondary tumors. Right: the statistical results of incidence for secondary tumor formation assay. Sorted cells represented isolated BTICs from MCF7 or MDA-MB-231 cells. All the data are presented as means  $\pm$  SD ( $n=3$ ). Asterisk indicates  $P < 0.05$ , compared with controls.

**Figure 4 The levels of TET1, TET3 and 5hmC in breast tumors are associated with intratumoral hypoxia, tumor malignant phenotypes and prognosis of patients with breast cancer.**

A, The expression of TET1 and TET3 as well as 5hmC level in *ductal carcinoma in situ* (DCIS) samples and grade I, grade II and grade III of *invasive ductal carcinoma* (IDC) samples. B, A significant correlation of TET1, TET3 and 5hmC levels with high grade DCIS and grade III of IDC. C, The expression of TET1 and TET3 as well as 5hmC level in invasive front of breast tumor. D and E, Overall survival (OS) and disease-free survival (DFS) analysis in 165 breast cancer cases showed a clinical significance of overexpression of TET1, TET3 or 5hmC in association with poor prognosis of patients with breast cancer. Negative group is referring to

non-overexpression of TET1, TET3 and 5hmC. The *P* values of the comparison are shown in the panel. Asterisk indicates  $P < 0.05$ . Double asterisk indicates  $P < 0.001$ .

**Figure 5 Genome-wide changes of 5hmC in response to hypoxia.**

A, Global level of 5hmC in MCF7 cells treated with hypoxia by dot blot assay. Methylene blue staining was used as a total genomic DNA loading control. B, Representative data showed the correlation of transcriptionally active (+) and inactive (-) compartment assignment based on Principal Component Analysis (PC1 values) and 5hmC change in a region of chromosome 1. C, Genome-wide comparison of Hi-C PC1 values with 5hmC change induced by hypoxia. D, Gene ontology results for the comparison of 5hmC change in hypoxia vs. normoxia. E, RNA-seq results show top ranked functional gene cluster correlated with hypoxia. F, Venn diagrams show the overlap between 5hmC correlated gene clusters and hypoxia associated gene clusters. The GO analysis results are shown in the bottom panel. G, hMeDIP-qPCR validation for the 5hmC change of TNF $\alpha$  gene. Two sets of primers targeting genome regions of TNF $\alpha$  gene were used, as indicated. H, The RNA polIII binding to TNF $\alpha$  gene was increased in hypoxia. N: normoxia H: hypoxia. All the data are presented as means  $\pm$  SD ( $n=3$ ). Asterisk indicates  $P < 0.05$ , compared with controls.

**Figure 6 Hypoxia induces TNF $\alpha$ -p38-MAPK signaling in breast cancer cells.**

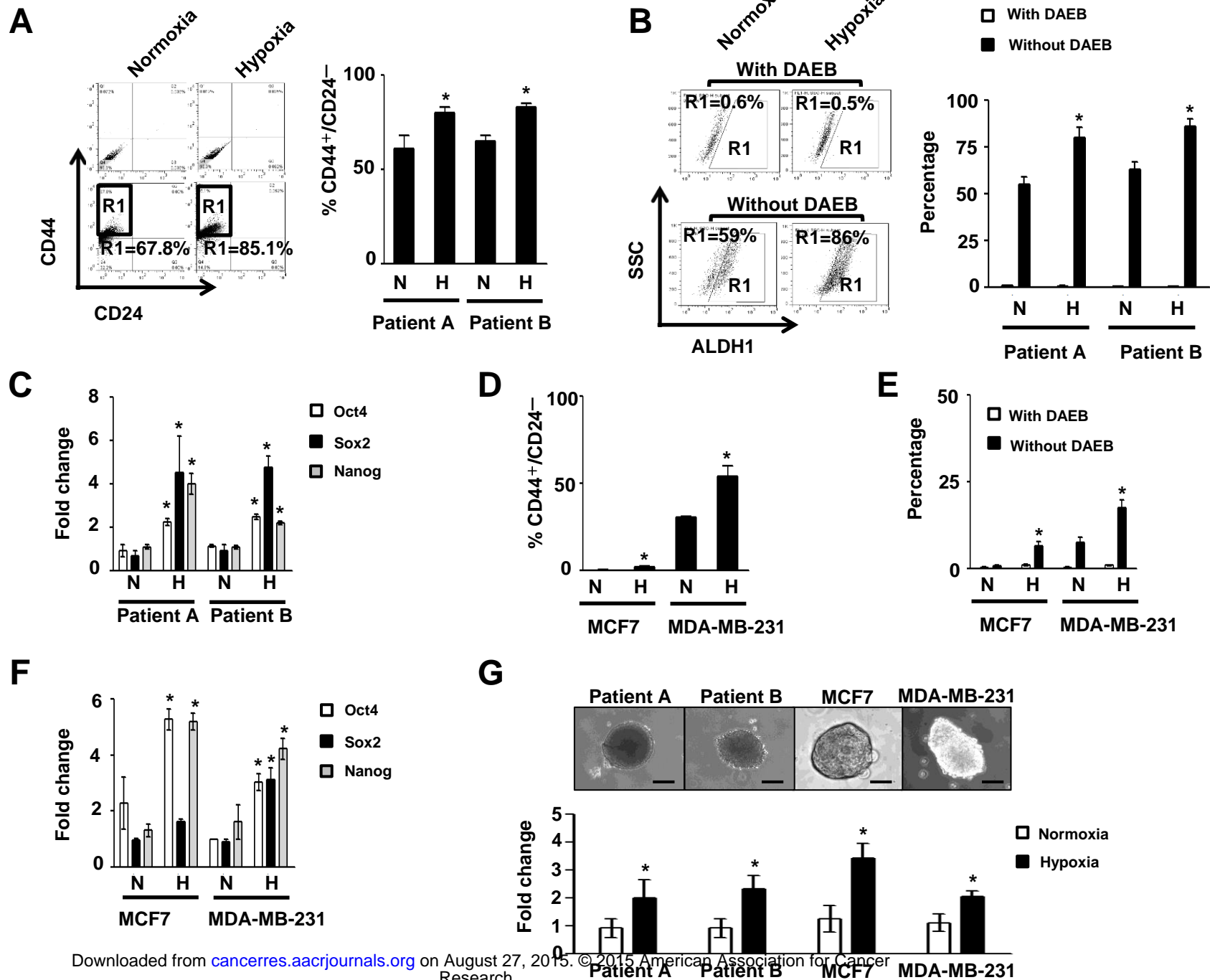
A, RT-qPCR analysis for TNF $\alpha$  gene expression in hypoxic primary breast cancer cells. B, Western blot analysis for protein level of TNF $\alpha$  and phospho-p38-MAPK in primary cells treated with hypoxia. C and D, Hypoxia increased expression of TNF $\alpha$  gene in mRNA level and protein level as well as the level of phospho-p38-MAPK in either MCF7 or MDA-MB-231 cells. E and F, Activation of TNF $\alpha$ -p38-MAPK signaling in either MCF7 or MDA-MB-231 HIF-1 $\alpha$  overexpression cells. RT-qPCR analysis (E) for TNF $\alpha$  gene expression and western blot analysis (F) for protein level of TNF $\alpha$  and phospho-p38-MAPK. G and H, The RT-qPCR analysis and western blot analysis showing TNF $\alpha$ -p38 MAPK signaling was activated in isolated BTICs. I, ELISA analysis showed an elevated level of secreted TNF $\alpha$  protein in hypoxic primary cells. J and K, The level of secreted TNF $\alpha$  protein was increased in hypoxic MCF7 or MDA-MB-231 cells as well as in their corresponding isolated BTICs. N: normoxia H: hypoxia. Sorted cells represented isolated BTICs from MCF7 or MDA-MB-231 cells. All the data are presented as means  $\pm$  SD ( $n=3$ ). Asterisk indicates  $P < 0.05$ , compared with controls.

**Figure 7 TNF $\alpha$ -p38-MAPK signaling is critical in maintaining BTIC capabilities.**

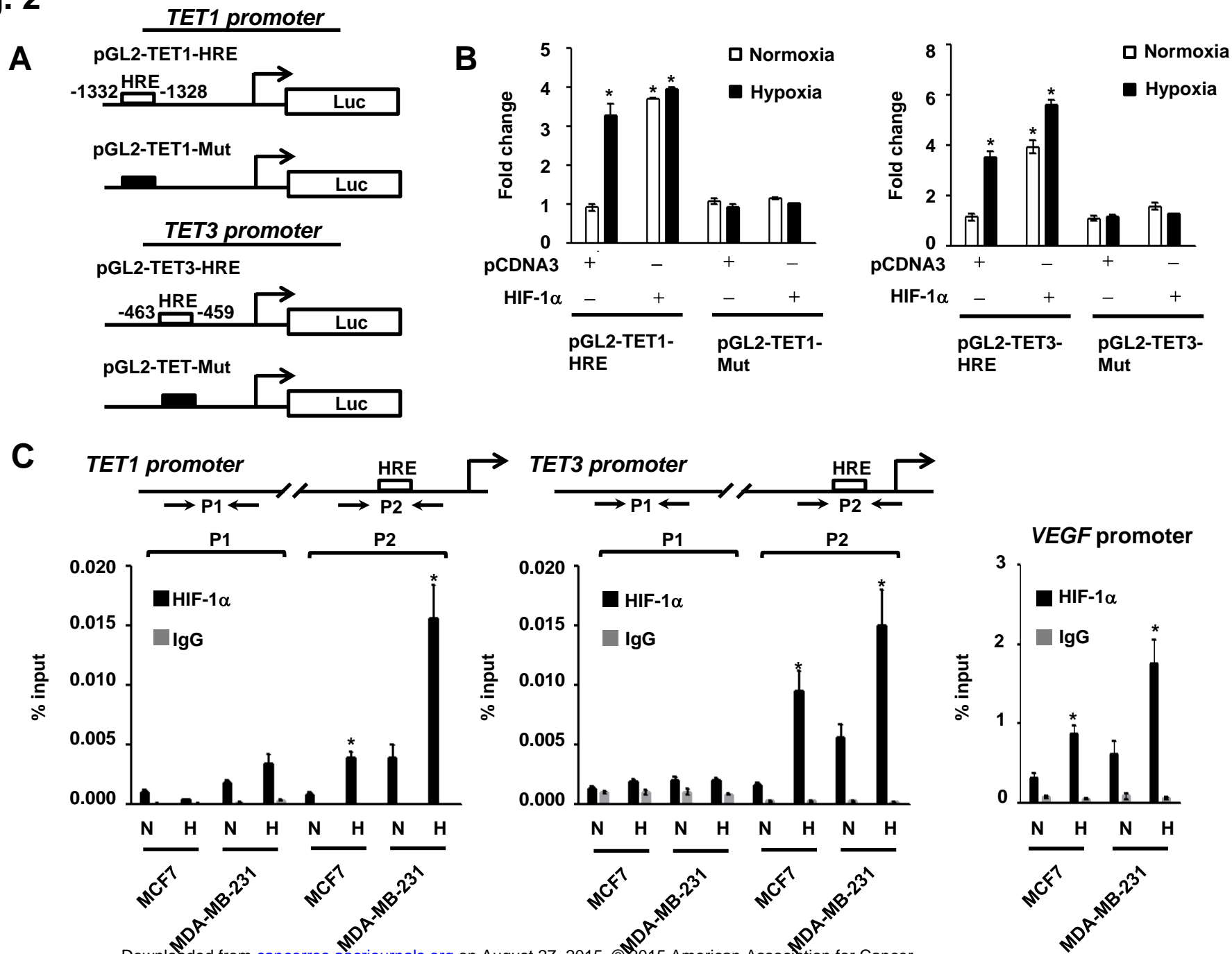
A, Treatment of anti- TNF $\alpha$  antibody (50 ng/ml or 100 ng/ml) reduced the

subpopulation of cells with CD44<sup>+</sup>/CD24<sup>-</sup> markers. B, Population of ALDEFLUOR-positive (ALDH<sup>+</sup>) cells was decreased in the treatment of anti-TNF $\alpha$  antibody (100 ng/ml). C, EMT process was reduced in isolated BTICs treated with anti-TNF $\alpha$  antibody. D, Down-regulation of TNF $\alpha$  reduced expression of stemness related genes in isolated BTICs. E and F, FACS analysis and ALDH1 enzyme activity assay showed that knocking down TNF $\alpha$  decreased the subpopulation of cells harboring putative BTIC markers. G, Western blot analysis showed a reduced EMT feature and p38 activation in TNF $\alpha$  knockdown cells. Control cells represented isolated BTICs without expressing shRNA. H, Sphere formation ability was reduced when TNF $\alpha$  was knocked down in isolated BTICs. Three rounds of spheroid formation assay were performed, as indicated. I, Knockdown of TNF $\alpha$  decreased drug resistance to paclitaxel treatment in isolated BTICs. J, xenograft study showed an inhibitory effect of TNF $\alpha$  knockdown on the tumor formation ability of isolated BTICs. Sorted cells represented isolated BTICs from MCF7 or MDA-MB-231 cells. All the data are presented as means  $\pm$  SD ( $n=3$ ). Asterisk indicates  $P < 0.05$ , compared with controls.

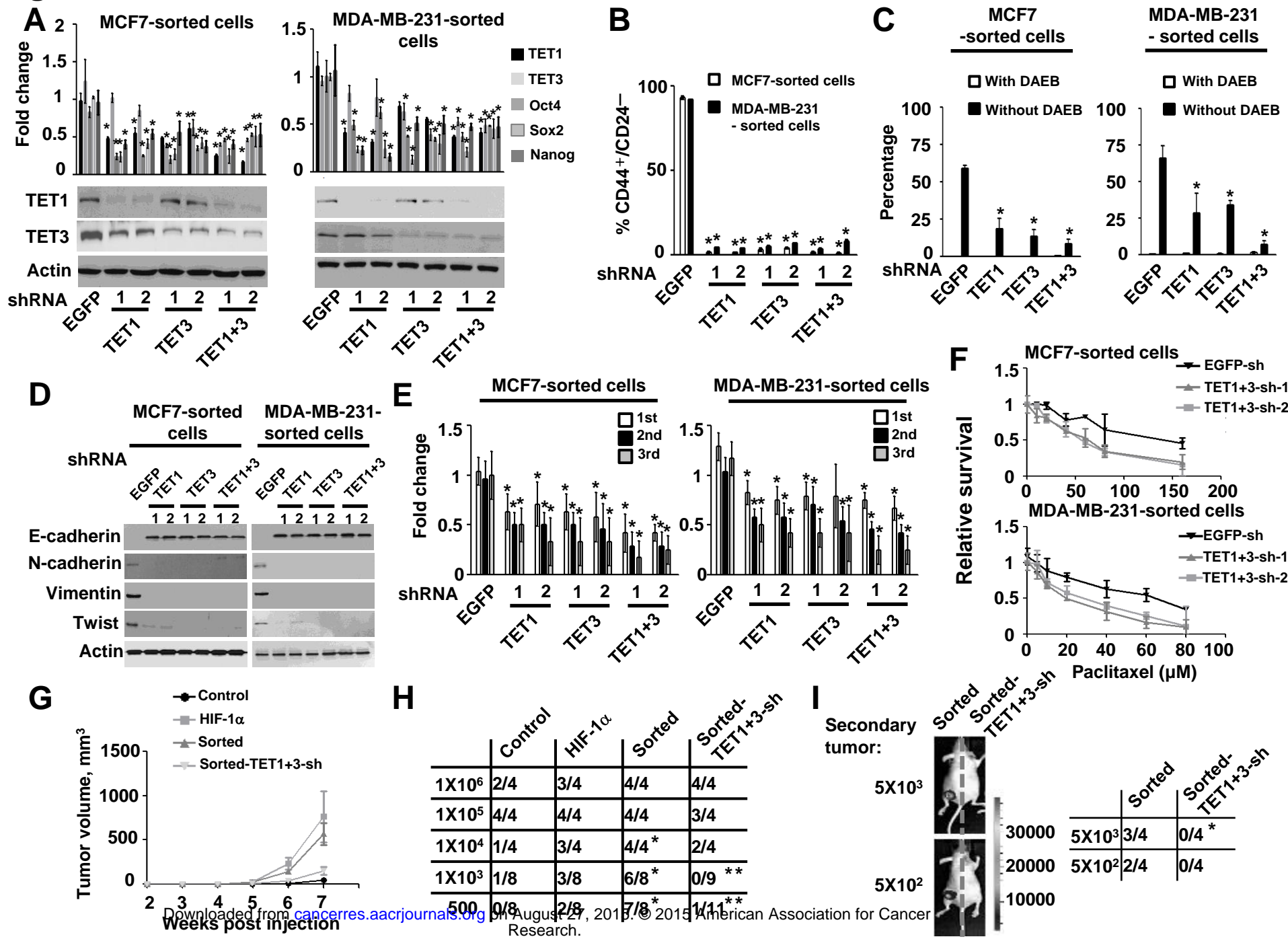
**Fig. 1**



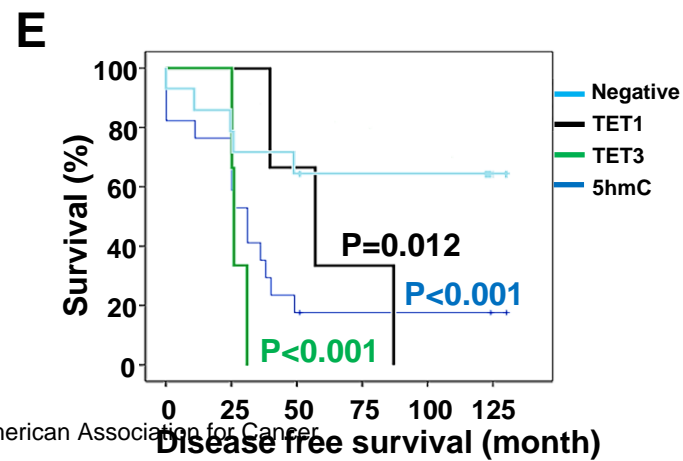
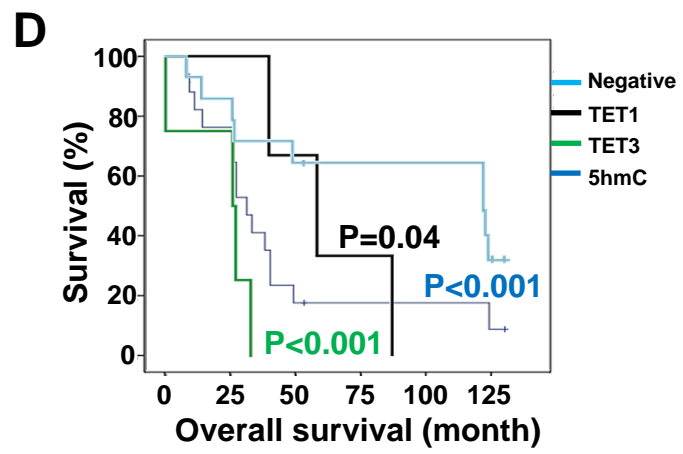
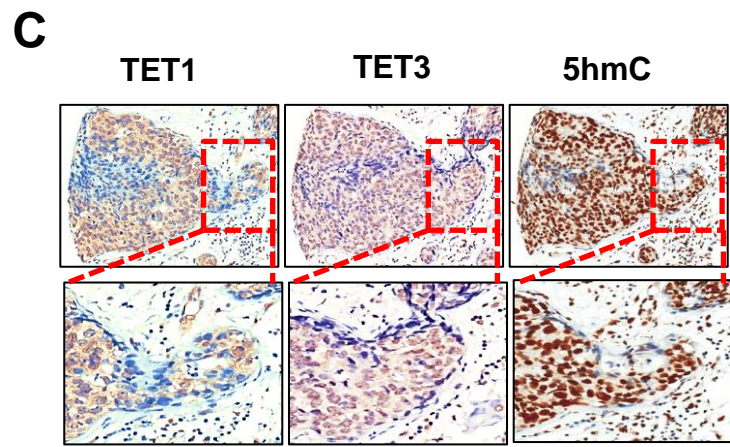
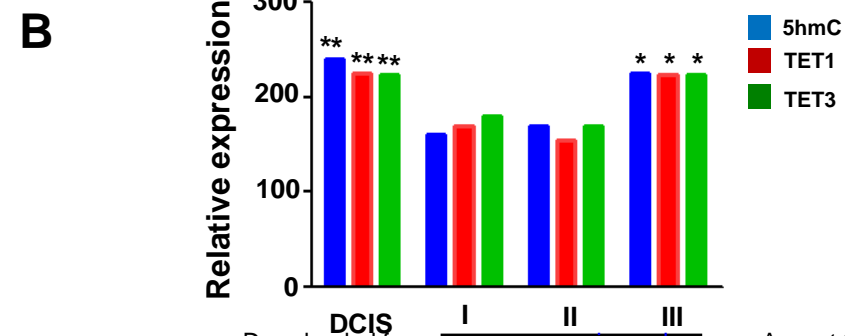
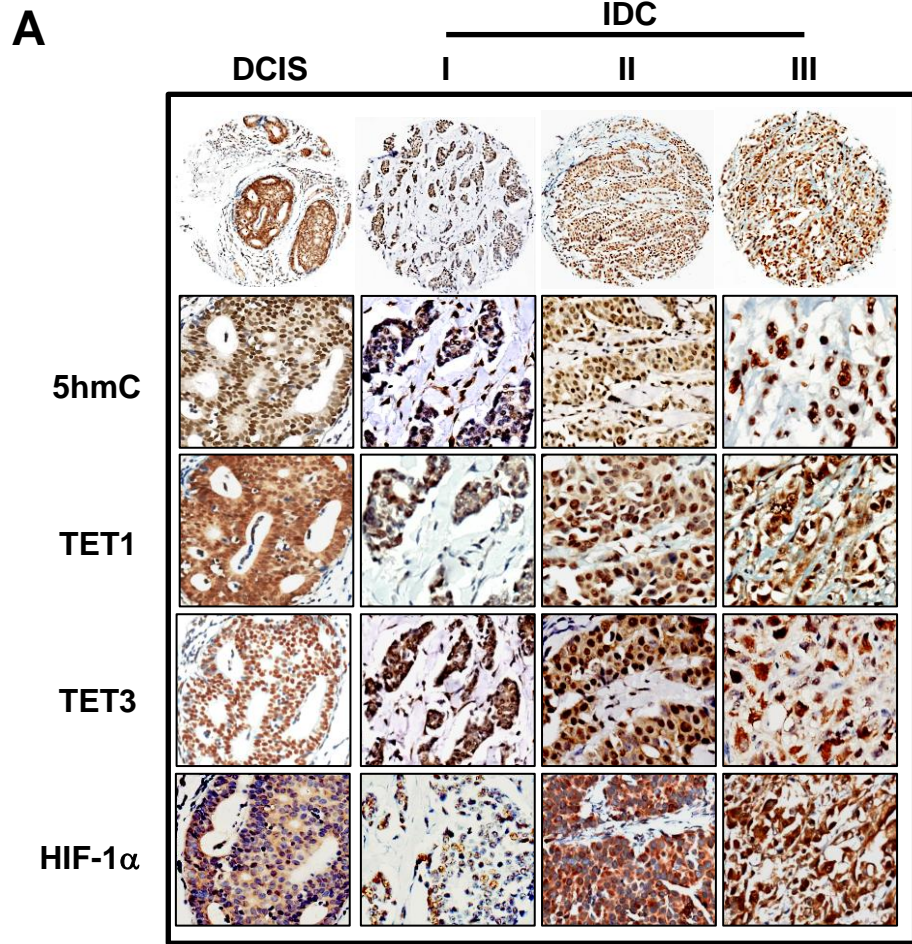
**Fig. 2**



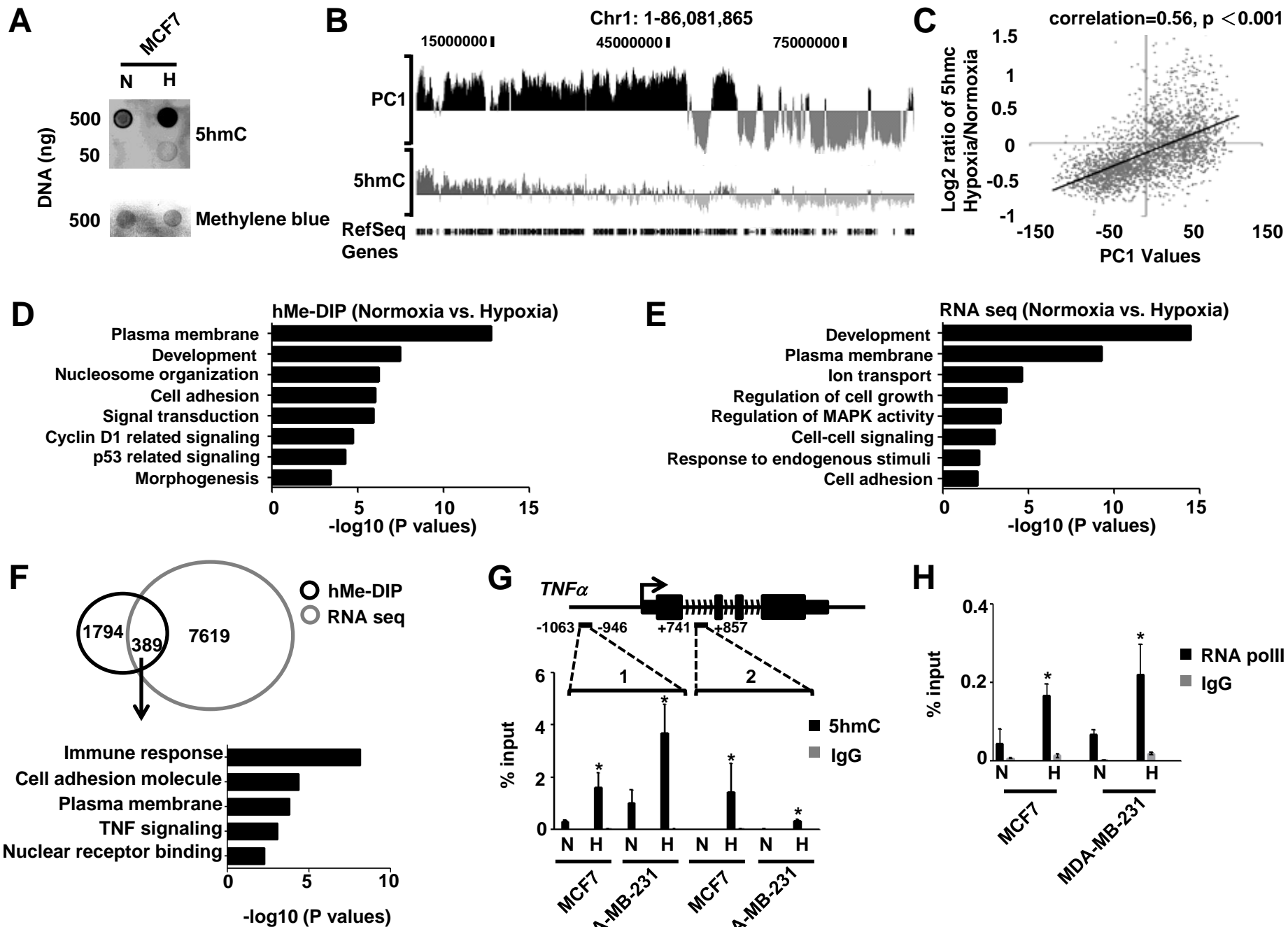
**Fig. 3**

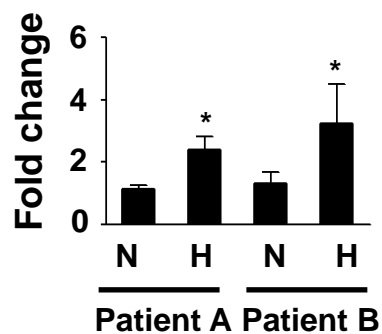
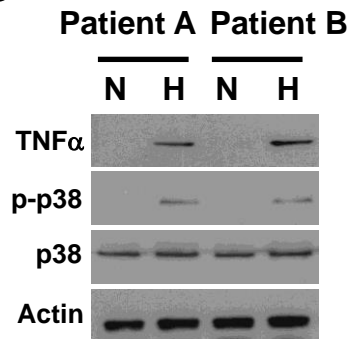
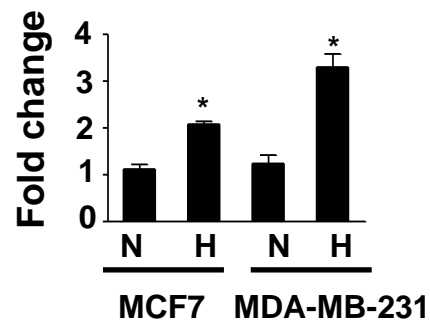
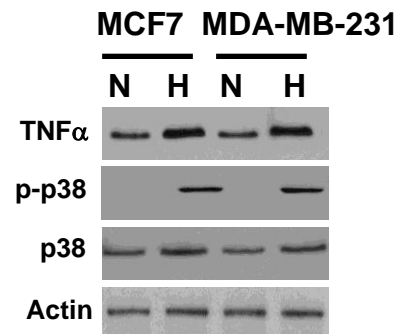
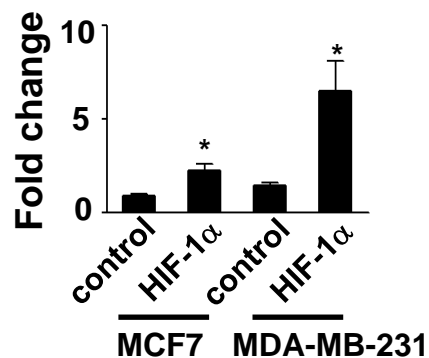
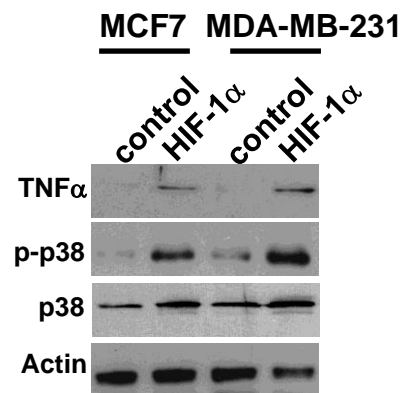
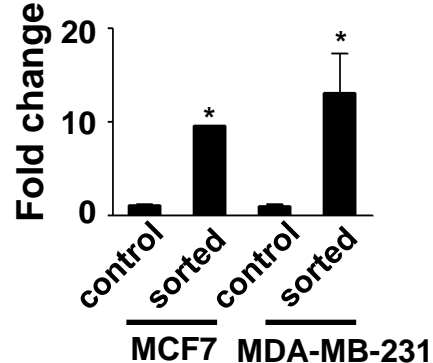
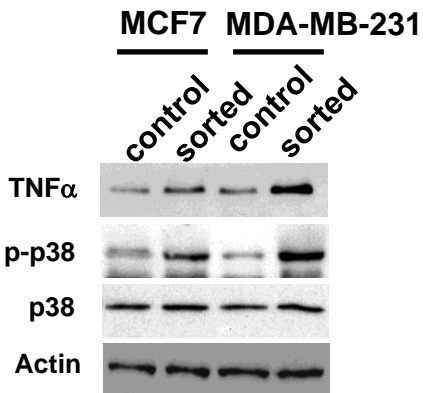
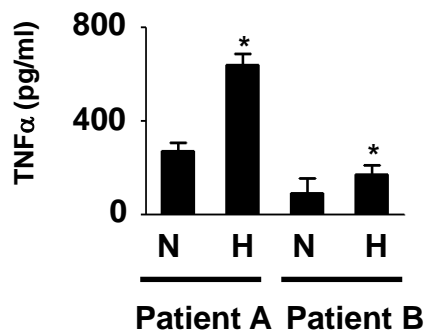
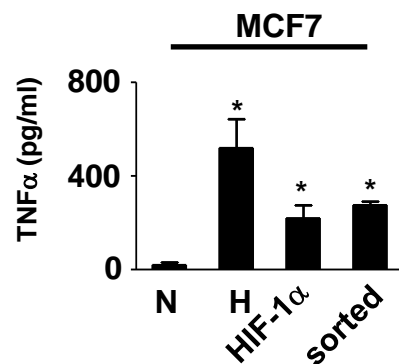
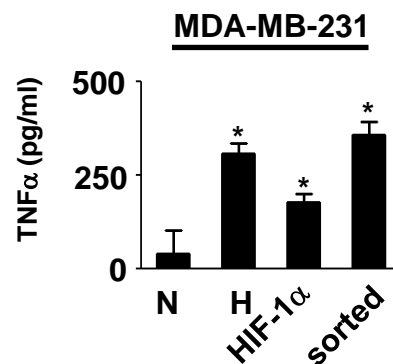


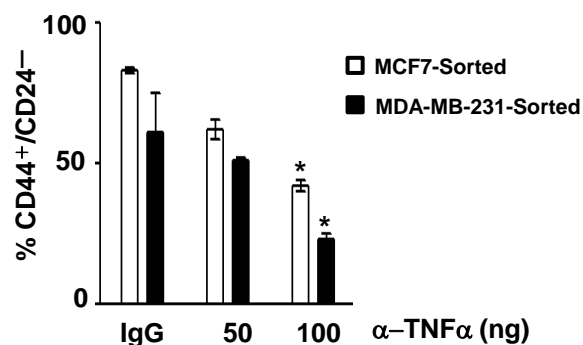
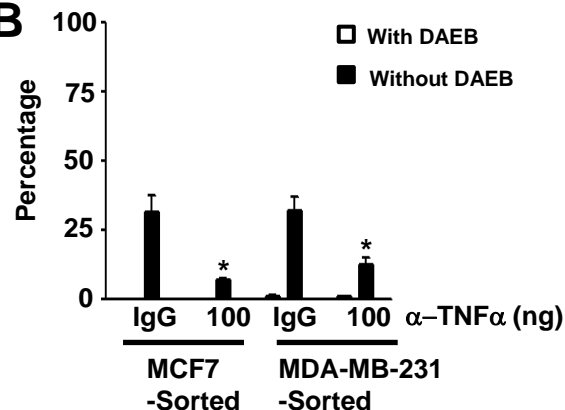
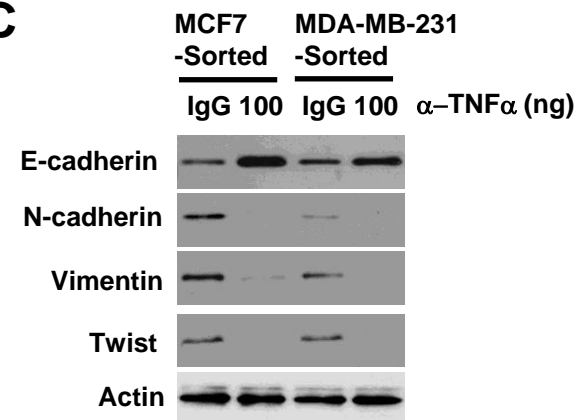
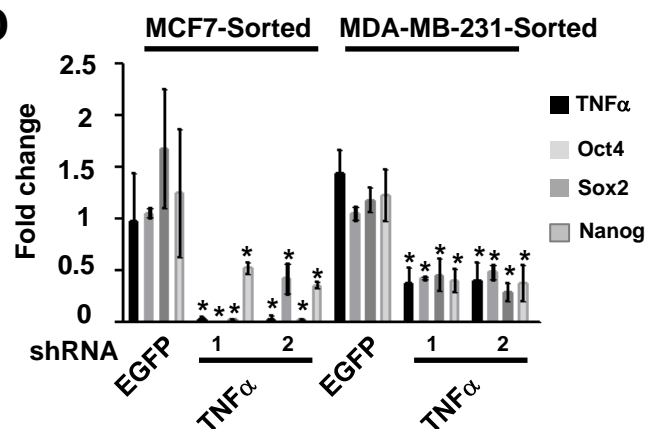
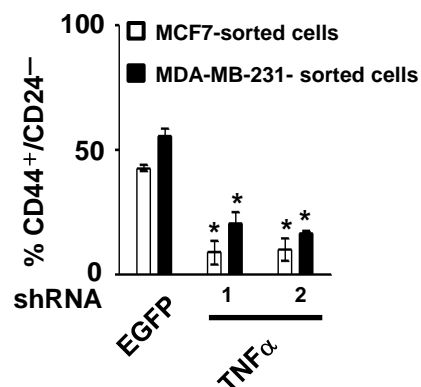
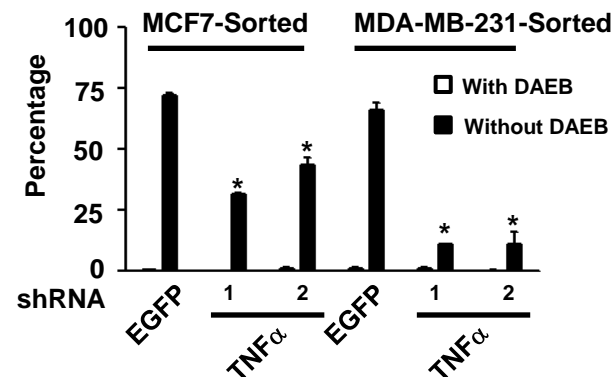
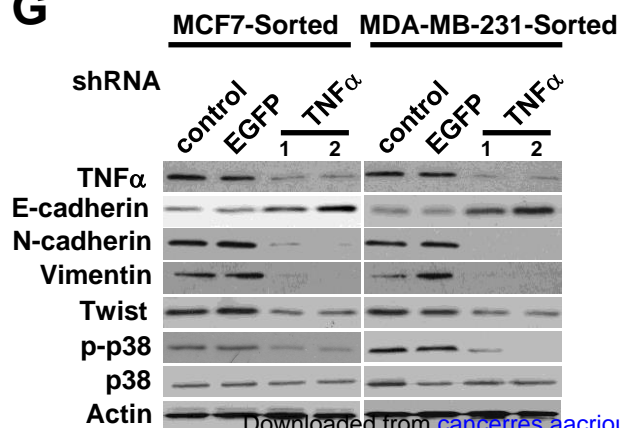
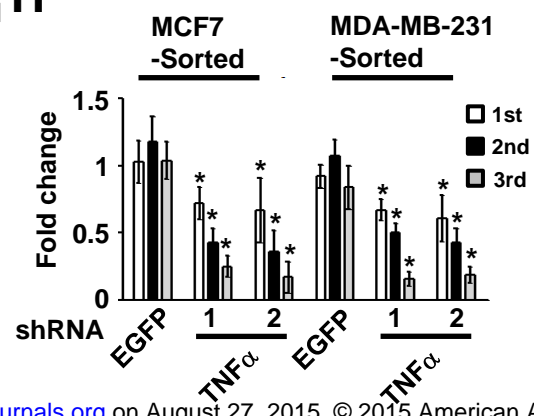
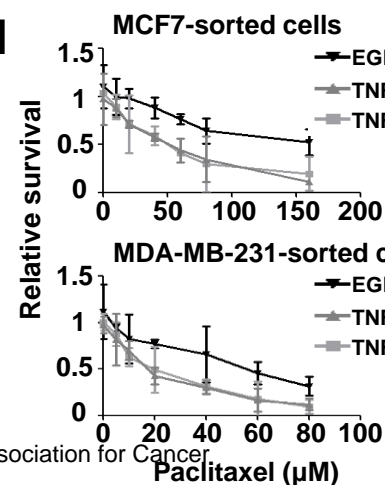
**Fig. 4**



**Fig. 5**



**Fig. 6****A****B****C****D****E****F****G****H****I****J****K**

**Fig. 7****A****B****C****D****E****F****G****H****I****J**

	EGFP-sh	TNFα-sh
1X10 <sup>6</sup>	2/4	1/4
1X10 <sup>5</sup>	4/4	1/4
1X10 <sup>4</sup>	4/4	0/4 *
1X10 <sup>3</sup>	5/10	0/10 *
500	6/10	0/10 *

# Cancer Research

The Journal of Cancer Research (1916–1930) | The American Journal of Cancer (1931–1940)

## Hypoxia drives breast malignancy through a TET -TNF $\alpha$ -p38-MAPK signaling axis

Min-Zu Wu, Su-Feng Chen, Shin Nieh, et al.

*Cancer Res* Published OnlineFirst August 20, 2015.

<b>Updated version</b>	Access the most recent version of this article at: doi: <a href="https://doi.org/10.1158/0008-5472.CAN-14-3208">10.1158/0008-5472.CAN-14-3208</a>
<b>Supplementary Material</b>	Access the most recent supplemental material at: <a href="http://cancerres.aacrjournals.org/content/suppl/2015/08/20/0008-5472.CAN-14-3208.DC1.html">http://cancerres.aacrjournals.org/content/suppl/2015/08/20/0008-5472.CAN-14-3208.DC1.html</a>
<b>Author Manuscript</b>	Author manuscripts have been peer reviewed and accepted for publication but have not yet been edited.

**E-mail alerts** [Sign up to receive free email-alerts](#) related to this article or journal.

**Reprints and Subscriptions** To order reprints of this article or to subscribe to the journal, contact the AACR Publications Department at [pubs@aacr.org](mailto:pubs@aacr.org).

**Permissions** To request permission to re-use all or part of this article, contact the AACR Publications Department at [permissions@aacr.org](mailto:permissions@aacr.org).